PNAS RESEARCH ARTICLE | IMMUNOLOGY AND INFLAMMATION

Autophagy induced by taurolidine protects against polymicrobial sepsis by promoting both host resistance and disease tolerance

Jie Huang[a,1], Michael Ita[b,1], Huiting Zhou[a,1], He Zhao[a], Fara Hassan[b], Zhenjiang Bai[a], D. Peter O'Leary[b], Yiping Li[a], H. Paul Redmond[b], Jiang Huai Wang[b,2], and Jian Wang[a,c,2]

Edited by Luis Moita, Instituto Gulbenkian de Ciência, Oeiras, Portugal; received December 31, 2021; accepted February 9, 2022 by Editorial Board Member Tak W. Mak

Sepsis, septic shock, and their sequelae are the leading causes of death in intensive care units, with limited therapeutic options. Disease resistance and tolerance are two evolutionarily conserved yet distinct defense strategies that protect the host against microbial infection. Here, we report that taurolidine administered at 6 h before septic challenge led to strong protection against polymicrobial sepsis by promoting both host resistance and disease tolerance characterized by accelerated bacterial clearance, ameliorated organ damage, and diminished vascular and gut permeability. Notably, taurolidine administered at 6 h after septic challenge also rescued mice from sepsis-associated lethality by enhancing disease tolerance to tissue and organ injury. Importantly, this in vivo protection afforded by taurolidine depends on an intact autophagy pathway, as taurolidine protected wild-type mice but was unable to rescue autophagy-deficient mice from microbial sepsis. In vitro, taurolidine induced light chain 3-associated phagocytosis in innate phagocytes and autophagy in vascular endothelium and gut epithelium, resulting in augmented bactericidal activity and enhanced cellular tolerance to endotoxin-induced damage in these cells. These results illustrate that taurolidine-induced autophagy augments both host resistance and disease tolerance to bacterial infection, thereby conferring protection against microbial sepsis.

autophagy | host resistance | disease tolerance | microbial sepsis

Sepsis is defined as a life-threatening organ dysfunction caused by a dysregulated host response to infection (1). Despite significant achievements in our understanding of the pathological and molecular basis of sepsis as well as the substantial improvement in diagnosis and supportive treatment over the last several decades, sepsis remains the leading cause of death in intensive care units and the third most common cause of overall hospital mortality worldwide (1, 2). Mortality rates of septic patients remain unacceptably high, ranging from 20 to 30% to up to 50 to 70% in septic shock (1, 3, 4). Furthermore, the incidence of sepsis and its associated economic burden continue to increase steadily by 1% every year (2, 5). Currently, the basic elements for the treatment of sepsis are limited largely to antibiotics, fluid resuscitation, oxygen, and support of organ function, with no clinically approved drugs that specifically target this disease (2, 6).

Upon bacterial infection, there are two evolutionarily conserved yet distinct defense strategies that protect the host against microbial threats (7, 8). One is the host resistance to infection, which relies on reducing microbial pathogen burden. The other is the disease tolerance to infection, which depends upon minimizing microbial infection-associated disease severity. The resistance strategy is a function of both innate and adaptive immunity and has been well studied and demonstrated (9–12). Concisely, the innate immune system responds rapidly through activation of pattern-recognition receptors (PRRs) upon detection of pathogen-associated molecular patterns, the highly conserved molecular structures of microbial pathogens (9). The transmembrane Toll-like receptors (TLRs) and cytoplasmic nucleotide-binding oligomerization domain (NOD)-like receptors (NLRs), in particular TLR2/4 and NOD1/2, are the best known PRRs that play a key role in host defense against microbial infection by activation of TLR- and/or NOD-mediated intracellular signal transduction pathways and initiation of both inflammatory and antimicrobial responses in innate phagocytes, which ultimately culminate in eliminating the invaded pathogens from the body (10–12). In contrast to the resistance strategy, disease tolerance does not directly affect microbial pathogen load; instead, it minimizes host vulnerability to cell and tissue damage caused by the microbial pathogens and/or by the immune response against them (7, 8). The concept of disease tolerance as a host defense strategy was originally demonstrated in

Significance

Disease resistance and tolerance are evolutionarily conserved yet distinct defense strategies that protect the host against microbial infection. Here, we report that taurolidine administered before the start of infection confers protection against polymicrobial sepsis by promoting resistance and tolerance. Notably, taurolidine given after the onset of infection also rescues mice from sepsis-associated lethality by enhancing disease tolerance to organ damage. This protection relies on an intact autophagy pathway, as taurolidine fails to protect autophagy-deficient mice against microbial sepsis. Specifically, taurolidine induces light chain 3-associated phagocytosis, but not xenophagy, in macrophages, resulting in an augmented bactericidal activity with enhanced cellular resistance to infection. These results highlight the importance of autophagy induction for taurolidine-augmented host resistance and disease tolerance and subsequent protection.

The authors declare no competing interest.

This article is a PNAS Direct Submission. L.M. is a guest editor invited by the Editorial Board.

[1]J.H., M.I., and H. Zhou contributed equally to this work.

[2]To whom correspondence may be addressed. Email: jh.wang@ucc.ie or wj196312@vip.163.com.

This article contains supporting information online at http://www.pnas.org/lookup/suppl/doi:10.1073/pnas.2121244119/-/DCSupplemental.

Published May 5, 2022.

plants (7, 13) and in *Drosophila* (7, 14), but was also recently reported in mammals subjected to *Plasmodium* infection (15) and severe polymicrobial sepsis (16). However, very little is currently known about the full spectrum of disease tolerance mechanisms.

Autophagy is a highly conserved intracellular process that delivers unwanted or damaged cytoplasmic components to lysosomes for degradation and recycling (17). This process involves the complex interplay of several autophagy-related (Atg) proteins that work in a coordinated manner with the de-novo-generated double-membrane-bound autophagosome to capture various targeted cytoplasmic materials, and these autophagosomes further fuse with lysosomes to form the degradative autolysosomes (18). Thus, autophagy functions as a ubiquitous eukaryotic cytoplasmic quality- and quantity-control mechanism by removing defective or surplus organelles and macromolecular aggregates to maintain the cellular homeostasis of the host (17, 18). Consequently, defects in the autophagic process can lead to inflammation and tissue damage, as evidenced by an established link between polymorphisms in the *Atg16L1* gene and predisposition to Crohn's disease (19). Moreover, autophagy has been discovered and demonstrated to act as an innate immune mechanism by sequestering and degrading intracellular pathogens for their targeted killing and destruction (18, 20), a process called xenophagy (21). Studies on several intracellular bacteria, in particular *Salmonella typhimurium*, underscore a crucial role of xenophagy in the restriction of bacterial replication (18, 22). Notably, microtubule-associated protein 1 light chain 3 (LC3)-associated phagocytosis (LAP), in addition to phagocytosis and xenophagy, constitutes the third pathway in innate phagocytes for engulfment and degradation of microbial pathogens (23–25). The process of LAP is characterized by the recruitment of LC3 to single-membrane-bound phagosomes, named LAPosomes, and combines the molecular machinery of autophagy with that of phagocytosis (25, 26). Thus, autophagy may possess an important role in host defense against microbial infection in the following two ways: one is its original role as a "self-eating" system for maintaining cellular homeostasis of the host; the other is a recently recognized role for autophagy to ingest and destroy the invaded microbial pathogens through xenophagy and LAP.

Taurolidine is a derivative of the semiessential amino acid taurine and was originally used in the treatment of patients with established peritonitis and catheter-related infections based on its antimicrobial properties (27, 28). In addition to its antimicrobial action, taurolidine has been shown to exert antineoplastic activity both in vitro and in vivo in a broad spectrum of tumor types (29–31). Importantly, one of the taurolidine-mediated cellular mechanisms is the induction of autophagy (31, 32). In the present study, we hypothesized that autophagy plays an important role in host defense against bacterial infection, and administration of taurolidine confers protection against microbial sepsis by promoting both host resistance and disease tolerance via autophagy induction. Here, we report that taurolidine protects mice against microbial sepsis via an augmented capacity of host resistance and disease tolerance, as represented by accelerated bacterial clearance, ameliorated organ damage, and diminished vascular and gut permeability. We further find that taurolidine-afforded protection is dependent on an intact autophagy pathway, as taurolidine fails to protect autophagy-deficient mice against microbial sepsis. Finally, we show that taurolidine induces LAP in phagocytic macrophages and autophagy in both pulmonary endothelial cells (PECs) and intestinal epithelial cells (IECs), thereby augmenting innate phagocyte-associated bactericidal activity and simultaneously attenuating endotoxin-induced cellular damage.

Results

Taurolidine Confers Protection against Microbial Sepsis by Augmenting Host Resistance and Disease Tolerance. We first examined whether administration of taurolidine, an antibacterial and antineoplastic agent, affords protection against sepsis-associated lethality using a murine model of cecal ligation and puncture (CLP)-induced high-grade polymicrobial sepsis. Taurolidine administered at 6 h before CLP resulted in a significantly improved survival from 14.3% seen in phosphate-buffered saline (PBS)-treated, CLP-challenged mice to 81.0% ($P = 0.0001$), whereas taurolidine administered at 6 h after CLP also rescued septic mice with an overall survival at 61.9% ($P = 0.0017$) (Fig. 1*A*). We next assessed the impact of taurolidine on innate-immunity-associated host resistance to microbial infection as represented by the systemic inflammatory response, bacterial clearance, and polymorphonuclear neutrophil (PMN) recruitment in the infected site. CLP-induced polymicrobial sepsis caused a substantial elevation in circulating proinflammatory cytokines with serum peak levels of TNF-α at 2 h and IL-6 at 6 h post-CLP (Fig. 1 *B* and *C*); however, administration of taurolidine at 6 h either before CLP (Fig. 1*B*) or after CLP (Fig. 1*C*) did not affect serum TNF-α and IL-6. Notably, taurolidine administered at 6 h before CLP significantly diminished bacterial counts in the circulation and visceral organs including the liver, spleen, and lungs at 12 and 24 h post-CLP ($P < 0.05$, $P < 0.01$ versus PBS-treated, CLP-challenged mice) (Fig. 1*D*), indicating an accelerated bacterial clearance. By contrast, taurolidine given at 6 h after CLP was unable to reduce bacterial burden in the circulation and visceral organs (Fig. 1*E*). Markedly increased PMN subpopulation, but not the macrophage subpopulation, in the peritoneal cavity, the infected site was observed at 6 and 12 h post-CLP (Fig. 1 *F* and *G*); however, taurolidine administered at 6 h either before CLP (Fig. 1*F*) or after CLP (Fig. 1*G*) demonstrated no effect on PMN recruitment into the peritoneal cavity.

We further assessed the influence of taurolidine on disease tolerance capacity as represented by the extent of organ damage and vascular and gut permeability upon septic challenges. We selected serum lactate dehydrogenase (LDH) as an indicator for lung and general cellular damage; creatine kinase (CK) as an indicator for muscle, heart, and brain damage; alanine aminotransferase (ALT) as an indicator for liver damage; and urea as an indicator for kidney damage. These parameters were measured at 18 and 36 h post-CLP to reflect injuries to these tissues and organs. Taurolidine administered at 6 h before CLP strongly attenuated CLP-induced elevations in serum levels of LDH, CK, ALT, and urea, close to the basal levels seen in mice subjected to sham-CLP (Fig. 2*A*), indicating alleviated tissue and organ injury. Surprisingly, taurolidine given at 6 h after CLP also significantly reduced serum LDH, CK, ALT, and urea levels at 18 and 36 h post-CLP ($P < 0.05$, $P < 0.01$ versus PBS-treated, CLP-challenged mice) (Fig. 2*B*). We next examined the effect of taurolidine on vascular and gut permeability. Significantly enhanced vascular permeability in the lungs, liver, and kidneys (Fig. 2 *C* and *D*) as well as increased gut permeability (Fig. 2 *E* and *F*) were observed at 12 and 24 h post-CLP. Taurolidine administered at 6 h before CLP substantially attenuated CLP-induced increases in both vascular (Fig. 2*C*) and gut (Fig. 2*E*) permeability. Notably, a significant reduction in either vascular (Fig. 2*D*) or gut (Fig. 2*F*) permeability was also observed in mice treated with taurolidine at 6 h after CLP ($P < 0.05$, $P < 0.01$ versus PBS-treated, CLP-challenged mice). These results suggest that in addition to administration

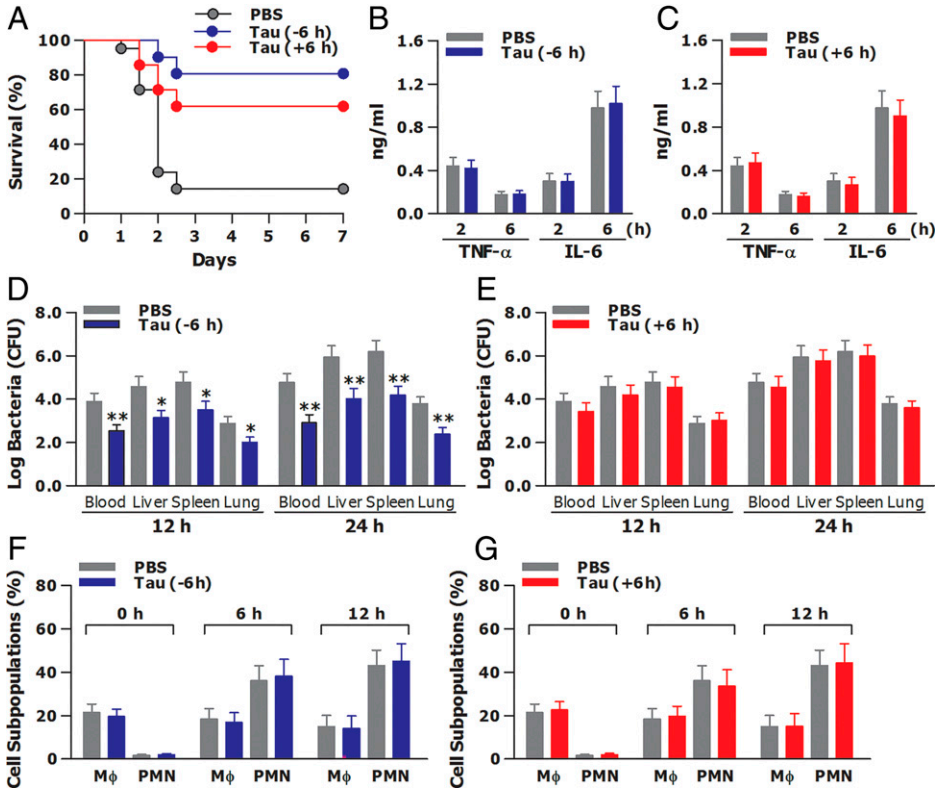

Fig. 1. Administration of taurolidine (Tau) protects mice against CLP-induced polymicrobial sepsis with accelerated bacterial clearance. C57BL/6 mice were subjected to CLP-induced high-grade polymicrobial sepsis and treated with Tau at 6 h before CLP (−6 h) or at 6 h after CLP (+6 h). (*A*) The Kaplan–Meier survival curve shows significantly improved survivals in mice that received Tau at 6 h either before CLP ($P = 0.0001$) or after CLP ($P = 0.0017$) compared to mice that received PBS ($n = 21$ per group). (*B* and *C*) Data shown are the results of serum TNF-α and IL-6 levels at 2 and 6 h post-CLP. (*D* and *E*) Bacterial counts in the blood and visceral organs including the liver, spleen, and lungs were assessed at 12 and 24 h post-CLP and expressed as log CFU/mL (*F* and *G*) Data shown are subpopulations (%) of macrophages ($CD11b^+F4/80^+CD11c^{lo}$) and PMNs ($CD11b^+F4/80^-Gr1^{hi}$) in the peritoneal lavage collected at 0, 6, and 12 h post-CLP. Data in *B* to *G* are mean ± SD ($n = 4$ to 6 mice per group for each time point). *$P < 0.05$, **$P < 0.01$ versus PBS-treated mice.

at 6 h before CLP, taurolidine administered even at 6 h after CLP still possesses an ability to enhance the capacity of disease tolerance, with ameliorated organ damage and attenuated vascular and gut permeability.

We next challenged mice with CLP-induced high-grade polymicrobial sepsis and treated them with antibiotics and fluid resuscitation at 3 h post-CLP to mimic the clinical scenario (33). Antibiotic administration plus fluid resuscitation prolonged the mean survival time in CLP-challenged mice from 44.7 h to 68.8 h ($P = 0.0217$) but failed to rescue them from sepsis-associated lethality, with identical mortality rates between mice that received antibiotics plus fluid resuscitation and mice that received no treatment (86.4 versus 85.7%) (*SI Appendix*, Fig. S1*A*). Notably, antibiotic administration plus fluid resuscitation substantially delayed bacterial spread into the circulation and visceral organs with reduced bacterial loads in the blood, liver, spleen, and lungs (*SI Appendix*, Fig. S1*B*). However, although the onset of organ damage and vascular and gut permeability was markedly delayed, antibiotic administration plus fluid resuscitation was unable to ameliorate sepsis-induced organ damage and vascular and gut permeability (*SI Appendix*, Fig. S1 *C*–*E*). We further examined whether taurolidine confers protection against sepsis-associated lethality in CLP-challenged, antibiotics-plus-fluid-resuscitation-treated mice. Taurolidine administered at 6 h before CLP or at 12 h after CLP significantly improved survival from 13.6% seen in CLP-challenged, antibiotics-plus-fluid-resuscitation-treated mice to 81.8% ($P = 0.0001$) or 63.6% ($P = 0.0007$) (*SI Appendix*, Fig. S2*A*). Notably, taurolidine given at 6 h before CLP (*SI Appendix*, Fig. S2*B*), but not at 12 h after CLP (*SI Appendix*, Fig. S2*C*), further reduced the already attenuated bacterial burden by antibiotic administration in the circulation and visceral organs. Importantly, taurolidine administered either at 6 h before CLP or at 12 h after CLP strongly ameliorated tissue and organ injury (*SI Appendix*, Fig. S2 *D* and *E*) and attenuated vascular and gut permeability (*SI Appendix*, Fig. S2 *F*–*I*) in septic mice. These results suggest that an augmented capacity of disease tolerance is predominantly responsible for taurolidine-afforded protection in CLP-challenged, antibiotics-plus-fluid-resuscitation-treated mice.

Taurolidine-Afforded Protection against Microbial Sepsis Is Dependent on an Intact Autophagy Pathway. We first asked whether deficiency in autophagy renders mice more susceptible to microbial infection. To test this, we used $LC3b^{-/-}$ mice, as these mice are deficient in LC3β (LC3B), a critical autophagy protein that participates in autophagosome formation and maturation, thus displaying reduced and destructive autophagy (34, 35). Wild-type and $LC3b^{-/-}$ mice were challenged with CLP-induced midgrade polymicrobial sepsis to assess their survival rates. $LC3b^{-/-}$ mice displayed an increased vulnerability with an overall mortality at 61.9% compared with a 33.3% mortality rate in wild-type mice ($P = 0.0463$) (Fig. 3*A*). While serum TNF-α and IL-6 levels (Fig. 3*B*) and PMN recruitment in the peritoneal cavity (Fig. 3*D*) upon septic challenge were comparable between wild-type and $LC3b^{-/-}$ mice, $LC3b^{-/-}$ mice showed increased bacterial counts in the blood, liver, spleen, and lungs at 12 h post-CLP ($P < 0.05$ versus wild-type mice) (Fig. 3*C*), indicating an impaired bacterial clearance. Furthermore, $LC3b^{-/-}$ mice displayed more severe tissue and

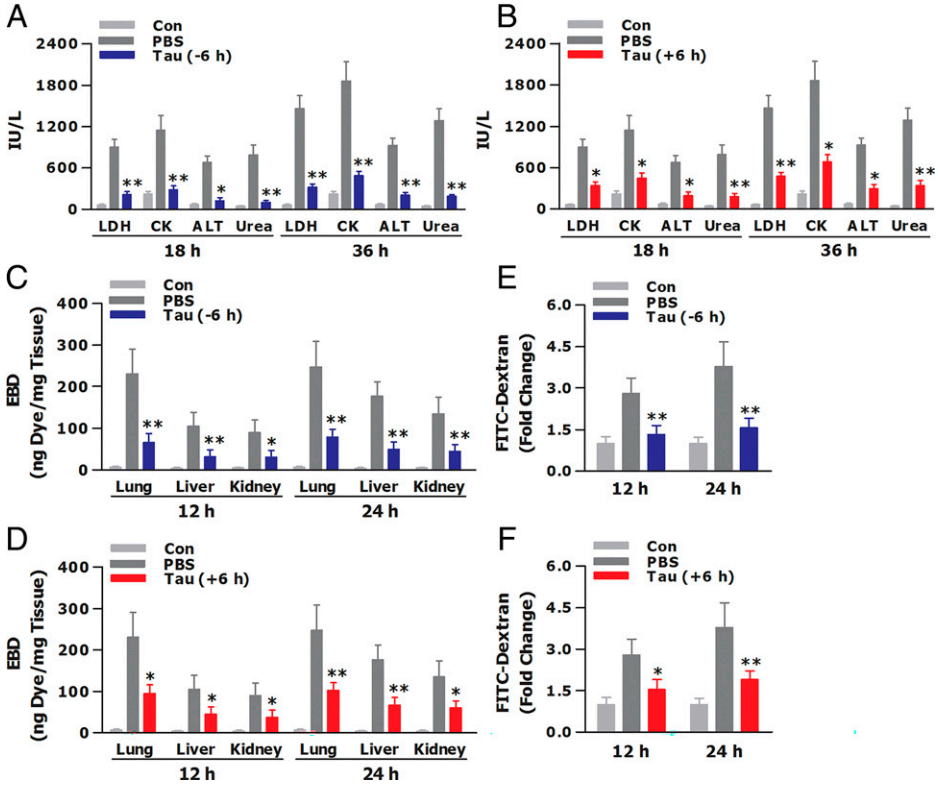

Fig. 2. Tau-afforded protection against microbial sepsis is associated with reduced organ damage and attenuated vascular and gut permeability. C57/BL6 mice were subjected to CLP-induced high-grade polymicrobial sepsis and treated with Tau at 6 h before CLP (−6 h) or at 6 h after CLP (+6 h). Mice subjected to sham-CLP were used as the control (Con). (*A* and *B*) Serum LDH, CK, ALT, and urea levels were assessed at 18 and 36 h post-CLP to reflect sepsis-induced tissue and organ injury. (*C* and *D*) Blood vascular permeability in the lungs, liver, and kidneys was assessed at 12 and 24 h post-CLP and expressed as nanograms of dye/milligram tissue. (*E* and *F*) Gut permeability was assessed at 12 and 24 h post-CLP and expressed as the fold change. Data are mean ± SD (n = 4 to 6 mice per group for each time point). *$P < 0.05$, **$P < 0.01$ versus PBS-treated mice.

organ injury with elevated serum LDH, CK, ALT, and urea at 18 h post-CLP compared to wild-type mice ($P < 0.05$) (Fig. 3*E*). Vascular (Fig. 3*F*) and gut (Fig. 3*G*) permeability at 12 h post-CLP in *LC3b*$^{-/-}$ mice were higher than those in wild-type mice ($P < 0.05$). To exclude a possibility that the observed vulnerability of *LC3b*$^{-/-}$ mice to CLP-induced polymicrobial sepsis is due to the difference in the cecal microbiome between autophagy-deficient mice and their wild-type littermates, we infected these mice with a combination of live gram-positive *Staphylococcus aureus* and gram-negative *Salmonella typhimurium*. *LC3b*$^{-/-}$ mice were more susceptible to bacterial infection with a much higher mortality rate than that in wild-type mice (68.3% versus 29.2%, $P = 0.0267$) (*SI Appendix*, Fig. S3*A*). Consistent with an increased overall mortality, *LC3b*$^{-/-}$ mice exhibited impaired bacterial clearance with increased bacterial loads in the circulation and visceral organs (*SI Appendix*, Fig. S3*B*). Moreover, *LC3b*$^{-/-}$ mice displayed aggravated organ damage (*SI Appendix*, Fig. S3*C*) and increased vascular and gut permeability (*SI Appendix*, Fig. S3 *D* and *E*) upon bacterial infection. Together, these results indicate that mice deficient in autophagy are more vulnerable to microbial infection, which may be associated with defective capacities in both host resistance and disease tolerance.

We next examined whether taurolidine-afforded protection against microbial sepsis relies predominantly on an intact autophagy pathway by using both wild-type and *LC3b*$^{-/-}$ mice subjected to CLP-induced midgrade polymicrobial sepsis. Taurolidine administered at 6 h before CLP afforded a 100% protection in CLP-challenged wild-type mice ($P = 0.0042$) (Fig. 4*A*) but failed to protect *LC3b*$^{-/-}$ mice against sepsis-associated lethality (Fig. 4*B*). We further assessed bacterial clearance, the extent of tissue and organ injury, and vascular and gut permeability to represent the capacity of host resistance and disease tolerance to microbial infection, as these parameters were greatly improved or ameliorated by taurolidine in a CLP-induced high-grade polymicrobial sepsis model (Figs. 1 and 2). Administration of taurolidine resulted in a substantially accelerated clearance of bacteria from the circulation and visceral organs at 12 h post-CLP in wild-type mice ($P < 0.05$, $P < 0.01$ versus PBS-treated, CLP-challenged wild-type mice) (Fig. 4*C*) but was unable to attenuate bacterial spread into the blood, liver, spleen, and lungs in *LC3b*$^{-/-}$ mice (Fig. 4*D*). Furthermore, significantly reduced serum LDH, CK, ALT, and urea at 18 h post-CLP was observed in taurolidine-treated wild-type mice ($P < 0.05$, $P < 0.01$ versus PBS-treated, CLP-challenged wild-type mice) (Fig. 4*E*), indicating improved organ functions, whereas taurolidine lost its ability to ameliorate sepsis-induced tissue and organ injury in *LC3b*$^{-/-}$ mice (Fig. 4*F*). Consistent with its failure to prevent bacterial spread and to alleviate organ damage in autophagy-deficient mice, administration of taurolidine was unable to prevent CLP-induced vascular (Fig. 4*H*) and gut (Fig. 4*J*) permeability in *LC3b*$^{-/-}$ mice, which is in sharp contrast to the effect taurolidine had on wild-type mice where taurolidine effectively attenuated the increase in both vascular (Fig. 4*G*) and gut (Fig. 4*I*) permeability.

To validate the above findings, we additionally used autophagy-deficient *Becn1*$^{+/-}$ mice, as these mice are deficient in beclin 1, an essential autophagy protein that directs both initiation phase and maturation-fusion phase during the formation of autolysosomes (34, 36), and we challenged them with CLP-induced midgrade polymicrobial sepsis. In contrast to a 100% protection afforded in wild-type mice, taurolidine

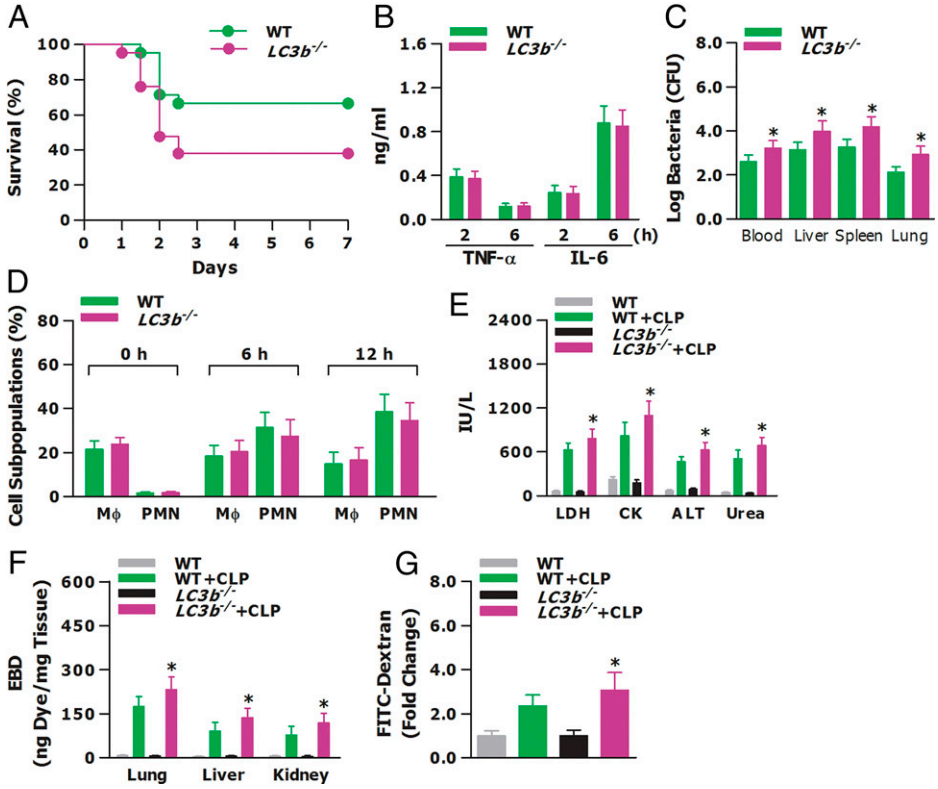

Fig. 3. Autophagy-deficient mice are susceptible to CLP-induced polymicrobial sepsis with impaired capacities in both host resistance and disease tolerance. Wild-type (WT) and *LC3b*$^{-/-}$ mice were subjected to CLP-induced midgrade polymicrobial sepsis. (*A*) The Kaplan–Meier survival curve shows that *LC3b*$^{-/-}$ mice were more vulnerable to microbial sepsis than their WT littermates ($P = 0.0463$) ($n = 21$ per group). (*B*) Data shown are the results of serum TNF-α and IL-6 levels at 2 and 6 h post-CLP. (*C*) Bacterial counts in the blood, liver, spleen, and lungs were assessed at 12 h post-CLP and expressed as log CFU/mL (*D*) Data shown are subpopulations (%) of macrophages ($CD11b^+F4/80^+CD11c^{lo}$) and PMNs ($CD11b^+F4/80^-Gr1^{hi}$) in the peritoneal lavage collected at 0, 6, and 12 h post-CLP. (*E*) Serum LDH, CK, ALT, and urea levels were assessed at 18 h post-CLP to reflect sepsis-induced tissue and organ injury. (*F*) Blood vascular permeability in the lungs, liver, and kidneys was assessed at 12 h post-CLP and expressed as nanograms of dye/milligram of tissue. (*G*) Gut permeability was assessed at 12 h post-CLP and expressed as fold change. Data in *B* to *G* are mean ± SD ($n = 4$ to 6 mice per group for each time point). *$P < 0.05$ versus CLP-challenged WT mice.

administered at 6 h before CLP was unable to rescue *Becn1*$^{+/-}$ mice from sepsis-associated lethality (*SI Appendix*, Fig. S4*A*). Administration of taurolidine in wild-type mice markedly diminished bacterial loads in the blood, liver, spleen, and lungs, indicating an augmented capacity of host resistance; however, taurolidine failed to attenuate bacterial spread into the circulation and visceral organs in *Becn1*$^{+/-}$ mice (*SI Appendix*, Fig. S4*B*). Furthermore, administration of taurolidine in wild-type mice augmented the capacity of disease tolerance with effectively ameliorated organ damage (*SI Appendix*, Fig. S4*C*) and reduced vascular and gut permeability (*SI Appendix*, Fig. S4 *D* and *E*), whereas these taurolidine-induced improvements were absent in *Becn1*$^{+/-}$ mice (*SI Appendix*, Fig. S4 *C–E*). We further examined whether taurolidine induces activation of the autophagy pathway in vivo by monitoring lipidation of LC3B in the visceral organs of CLP-challenged wild-type mice and found that taurolidine administered at 6 h before CLP resulted in LC3B lipidation with increased expression of LC3B-II in the lungs, liver, and kidneys at 6 and 18 h post-CLP (*SI Appendix*, Fig. S4*F*). Collectively, these results indicate that taurolidine-afforded protection against microbial sepsis via promotion of both host resistance and disease tolerance is dependent on an intact autophagy pathway.

Taurolidine Enhances Innate Phagocyte-Associated Bactericidal Activity via Initiation of LAP in Macrophages. We first examined whether taurolidine induces autophagy in innate phagocytes and subsequently augments antimicrobial activity in these cells. Macrophages isolated from wild-type mice were treated with culture medium (CM) or taurolidine and further challenged with *S. aureus* and *S. typhimurium* to assess bacterial phagocytosis and intracellular killing of the ingested bacteria. Treatment of macrophages with taurolidine resulted in a substantial increase in autophagy induction ($P < 0.01$ versus CM-treated macrophages) (Fig. 5*A* and *B*). Furthermore, taurolidine-treated macrophages displayed an augmented bactericidal activity with significantly increased phagocytosis (Fig. 5*C*) and intracellular killing (Fig. 5*D*) of *S. aureus* and *S. typhimurium*. To ascertain whether the augmented bactericidal activity in taurolidine-treated macrophages is primarily dependent on autophagy induction, macrophages isolated from wild-type and *LC3b*$^{-/-}$ mice were incubated with either PBS or 3-methyladenine (3-MA), an autophagy inhibitor that blocks autophagosome formation via its inhibitory effect on class III phosphatidylinositol 3-kinases (37), for 2 h, then treated with CM or taurolidine, and further challenged with *S. aureus* and *S. typhimurium*. Inhibition of autophagy in wild-type macrophages by 3-MA substantially attenuated taurolidine-induced augmentation in both phagocytosis (Fig. 5*E*) and intracellular killing (Fig. 5*F*) of *S. aureus* and *S. typhimurium*. Moreover, deficiency in autophagy almost completely abolished taurolidine-augmented bactericidal activity as evidenced by abrogated bacterial ingestion (Fig. 5*E*) and killing (Fig. 5*F*) in taurolidine-treated *LC3b*$^{-/-}$ macrophages. We further isolated peritoneal macrophages from PBS-treated or taurolidine-treated, CLP-challenged wild-type and *LC3b*$^{-/-}$ mice and

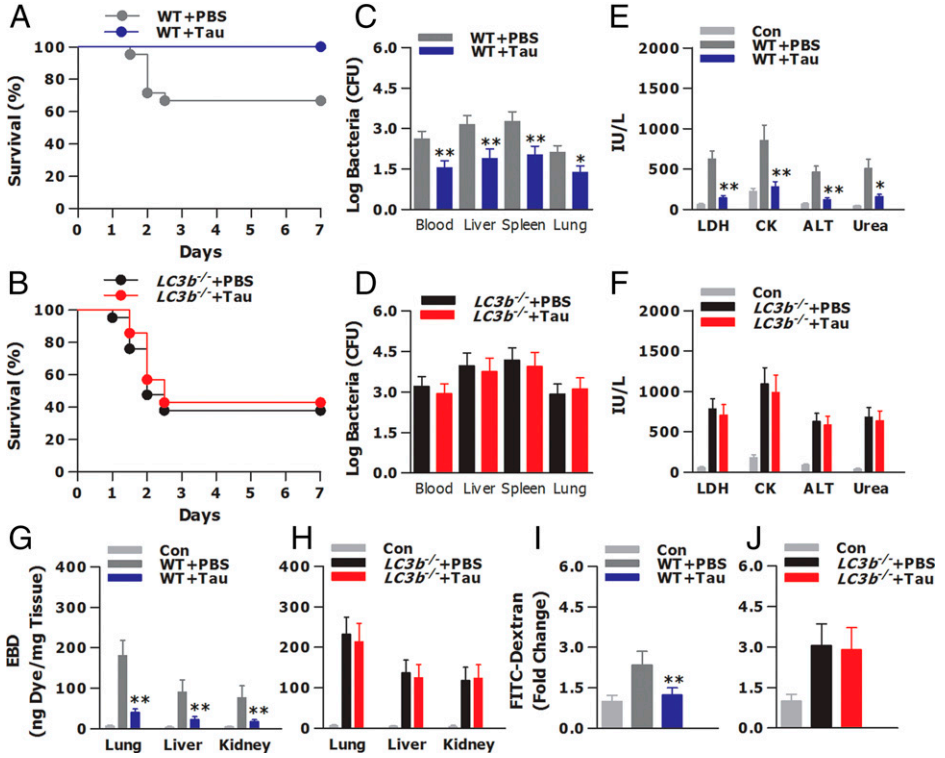

Fig. 4. Tau-afforded protection against microbial sepsis depends on an intact autophagy pathway. WT and *LC3b*$^{-/-}$ mice were subjected to CLP-induced midgrade polymicrobial sepsis and treated with Tau at 6 h before CLP. Mice subjected to sham-CLP were used as the Con. (*A* and *B*) The Kaplan–Meier survival curves show that administration of Tau confers a 100% protection in WT mice ($P = 0.0042$) but fails to protect *LC3b*$^{-/-}$ mice from sepsis-associated lethality ($P = 0.5921$) ($n = 21$ per group). (*C* and *D*) Bacterial counts in the blood, liver, spleen, and lungs were assessed at 12 h post-CLP and expressed as log CFU/mL. (*E* and *F*) Serum LDH, CK, ALT, and urea levels were assessed at 18 h post-CLP to reflect sepsis-induced tissue and organ injury. (*G* and *H*) Blood vascular permeability in the lungs, liver, and kidneys was assessed at 12 h post-CLP and expressed as nanograms of dye/milligram of tissue. (*I* and *J*) Gut permeability was assessed at 12 h post-CLP and expressed as the fold change. Data in *C*–*J* are mean ± SD ($n = 4$ to 6 mice per group). *$P < 0.05$, **$P < 0.01$ versus PBS-treated WT or *LC3b*$^{-/-}$ mice.

infected them with *S. aureus* and *S. typhimurium* to assess ex vivo bacterial phagocytosis and intracellular killing. Macrophages isolated from taurolidine-treated, CLP-challenged wild-type mice displayed strong engulfment (Fig. 5*G*) and killing (Fig. 5*H*) of *S. aureus* and *S. typhimurium* ($P < 0.05$, $P < 0.01$ versus macrophages isolated from PBS-treated, CLP-challenged wild-type mice), whereas macrophages isolated from taurolidine-treated, CLP-challenged *LC3b*$^{-/-}$ mice exhibited severe impairment in their bactericidal activity (Fig. 5 *G* and *H*), suggesting the importance of autophagy in the taurolidine-augmented capacity of cellular resistance in macrophages.

We next examined whether taurolidine is capable of initiating LAP in innate phagocytes. Macrophages isolated from wild-type mice were treated with CM or taurolidine and further challenged with *S. aureus* and *Escherichia coli* to assess the recruitment of LC3 to bacterium-containing phagosomes. Treatment of macrophages with taurolidine resulted in an apparent recruitment of LC3 to the phagosomes containing either *S. aureus* or *E. coli* (Fig. 6*A*), accounting for ∼38% colocalization of *S. aureus*-containing phagosomes and 41% colocalization of *E. coli*-containing phagosomes with LC3 at 60 min after bacterial uptake (Fig. 6*B*), whereas no obvious recruitment of LC3 to either *S. aureus*- or *E. coli*-containing phagosomes was observed in CM-treated macrophages (Fig. 6 *A* and *B*). We further isolated phagosomes from CM-treated or taurolidine-treated, *E. coli*-challenged wild-type macrophages to detect the recruited LC3 in these phagosomes. The presence of lysosome-associated membrane protein 1 (LAMP-1) and undetectable accumulations of both the cytosolic and endoplasmic reticulum markers β-tubulin and protein disulfide isomerase (PDI) demonstrated the purity of phagosome isolation (Fig. 6*C*). Notably, LC3B-II, the lipidated form of LC3B, was detected in the phagosomes from taurolidine-treated macrophages, but not from CM-treated macrophages (Fig. 6*C*). Furthermore, Rubicon, a RUN-domain-containing protein critically required for LAP, but not for xenophagy (25, 38), was detected only in the phagosomes isolated from taurolidine-treated macrophages (Fig. 6*C*), indicating that taurolidine induces LAP specifically in innate phagocytes. To determine whether LAP is predominantly responsible for taurolidine-augmented bactericidal activity, we knocked down either Rubicon or Ulk1 in wild-type macrophages. As shown in Fig. 6*D*, silencing Rubicon almost completely abated taurolidine-enhanced intracellular killing of *S. aureus* and *S. typhimurium* ($P < 0.01$ versus scrambled siRNA (scrRNA)-incubated, taurolidine-treated macrophages), whereas silencing Ulk1, which is essential for xenophagy but dispensable for LAP (26, 39), did not affect taurolidine-augmented bactericidal activity. In addition to Rubicon, LAP also depends upon NADPH oxidase and reactive oxygen species (ROS) (24, 38). We further used macrophages isolated from *Nox2*$^{-/-}$ mice, as these mice are deficient in gp91^{phox}, a NADPH oxidase catalytic core (40), and found that the capability of taurolidine-induced augmentation in bacterial killing was severely impaired in *Nox2*$^{-/-}$ macrophages ($P < 0.01$ versus taurolidine-treated wild-type macrophages) (Fig. 6*E*). Similarly, blockage of ROS generation by diphenyleneiodonium (DPI) substantially attenuated taurolidine-enhanced bactericidal activity ($P < 0.05$ versus taurolidine-treated wild-type macrophages) (Fig. 6*E*). Together, these results highlight a crucial requirement for taurolidine-initiated LAP in innate

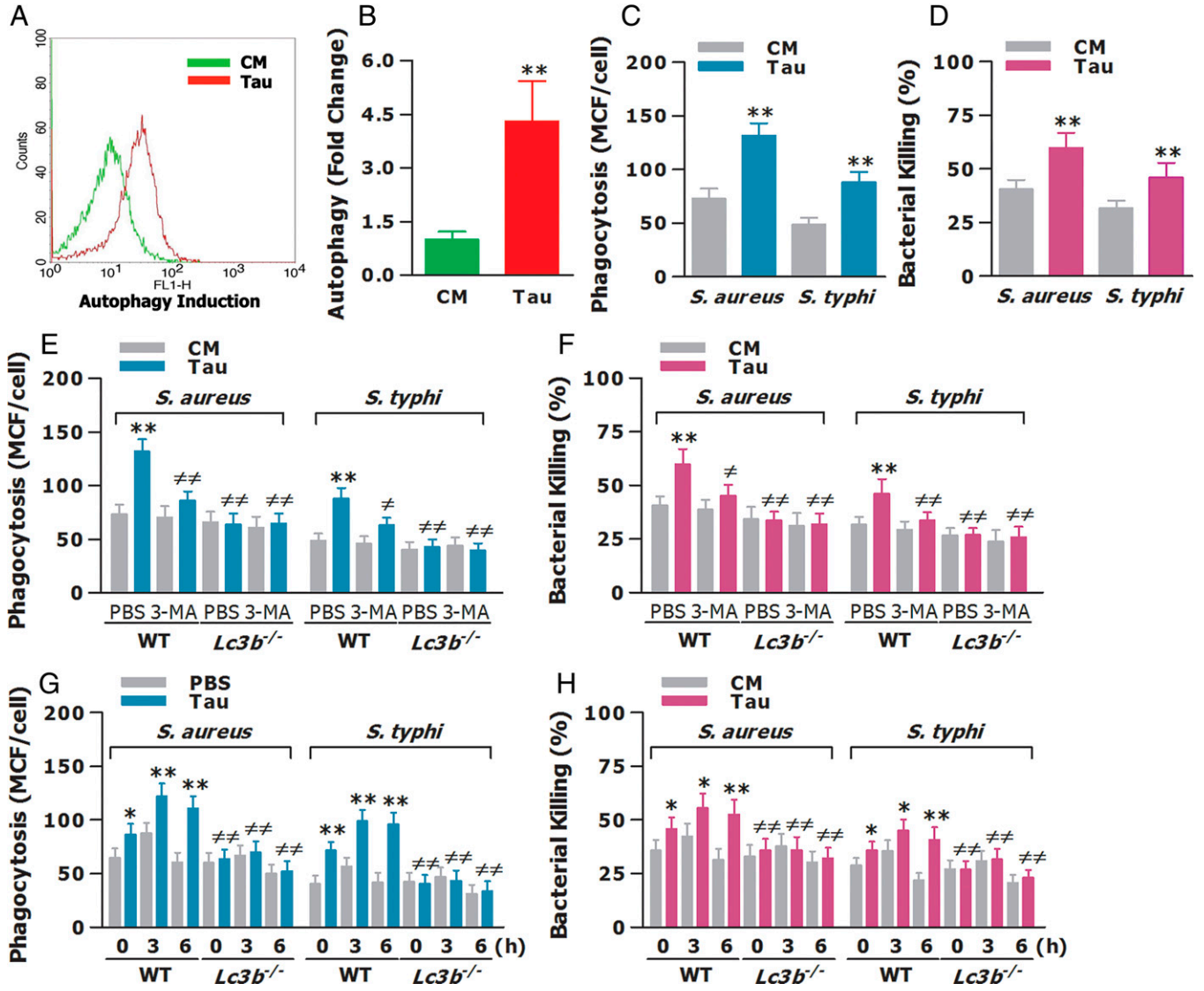

Fig. 5. Tau-induced autophagy in innate phagocytes enhances their resistance capacity with augmented bactericidal activity. (*A–D*) Isolated macrophages were treated with CM or Tau (50 μM) for 12 h to induce autophagy (*A* and *B*) and further challenged with FITC-conjugated or live *S. aureus* and *S. typhimurium* to assess bacterial phagocytosis (*C*) and intracellular killing (*D*). (*E* and *F*) Macrophages isolated from WT and *LC3b*$^{-/-}$ mice were incubated with PBS or 3-MA (5.0 mM) for 2 h, then treated with CM or Tau for 12 h, and further challenged with FITC-conjugated or live *S. aureus* and *S. typhimurium* to assess bacterial phagocytosis (*E*) and intracellular killing (*F*). (*G* and *H*) WT and *LC3b*$^{-/-}$ mice were subjected to CLP-induced polymicrobial sepsis and treated with PBS or Tau at 6 h before CLP. Peritoneal macrophages isolated at 0, 3, and 6 h post-CLP were further challenged with FITC-conjugated or live *S. aureus* and *S. typhimurium* to assess bacterial phagocytosis (*G*) and intracellular killing (*H*). Autophagy induction and bacterial phagocytosis were expressed as the fold change and mean channel fluorescence (MCF) per cell, respectively. Data in *B* to *H* are mean ± SD (n = 4 to 6 in duplicate or in triplicate). *P < 0.05, **P < 0.01 versus PBS-incubated, CM-treated WT macrophages or macrophages isolated from PBS-treated WT mice; $^{\neq}P$ < 0.05, $^{\neq\neq}P$ < 0.01 versus PBS-incubated, Tau-treated WT macrophages or macrophages isolated from Tau-treated WT mice.

phagocytes to enhance bactericidal activity, thereby augmenting the capacity of cellular resistance to microbial infection.

Taurolidine Induces Autophagy in Both PECs and IECs and Enhances Their Disease Tolerance to LPS-Induced Cellular Damage. We first determined whether taurolidine is capable of inducing autophagy in vascular endothelium and gut epithelium, thus promoting an enhanced capacity of disease tolerance to lipopolysaccharide (LPS)-induced cellular damage. Primary murine PECs and IECs isolated from wild-type mice were treated with CM or taurolidine and further challenged with PBS or LPS to assess LPS-induced cell death and disruption of the endothelial or epithelial monolayer integrity. Treatment with taurolidine induced a significant increase in autophagy formation in PECs (P < 0.01 versus CM-treated PECs) (Fig. 7*A* and *B*). Of note, PECs, when challenged with LPS, displayed markedly increased cell death with nearly 50% cell apoptosis (Fig. 7*C*) and substantially enhanced permeability of the endothelial monolayer (Fig. 7*D*); treatment with taurolidine strongly attenuated LPS-induced cell apoptosis and disruption of the endothelial monolayer (Fig. 7 *C* and *D*) (P < 0.01 versus CM-treated, LPS-challenged PECs). Similar results were also found in IECs where treatment of IECs with taurolidine resulted in a significant increase in autophagy induction (P < 0.01 versus CM-treated IECs) (Fig. 7 *E* and *F*), and furthermore, these taurolidine-treated IECs were characterized with significantly improved cell viability (Fig. 7*G*) and markedly attenuated permeability of the epithelial monolayer (Fig. 7*H*) in response to LPS challenge (P < 0.01 versus CM-treated, LPS-challenged IECs).

Next, we attempted to clarify whether taurolidine-induced autophagy is critical for an augmented capacity of disease

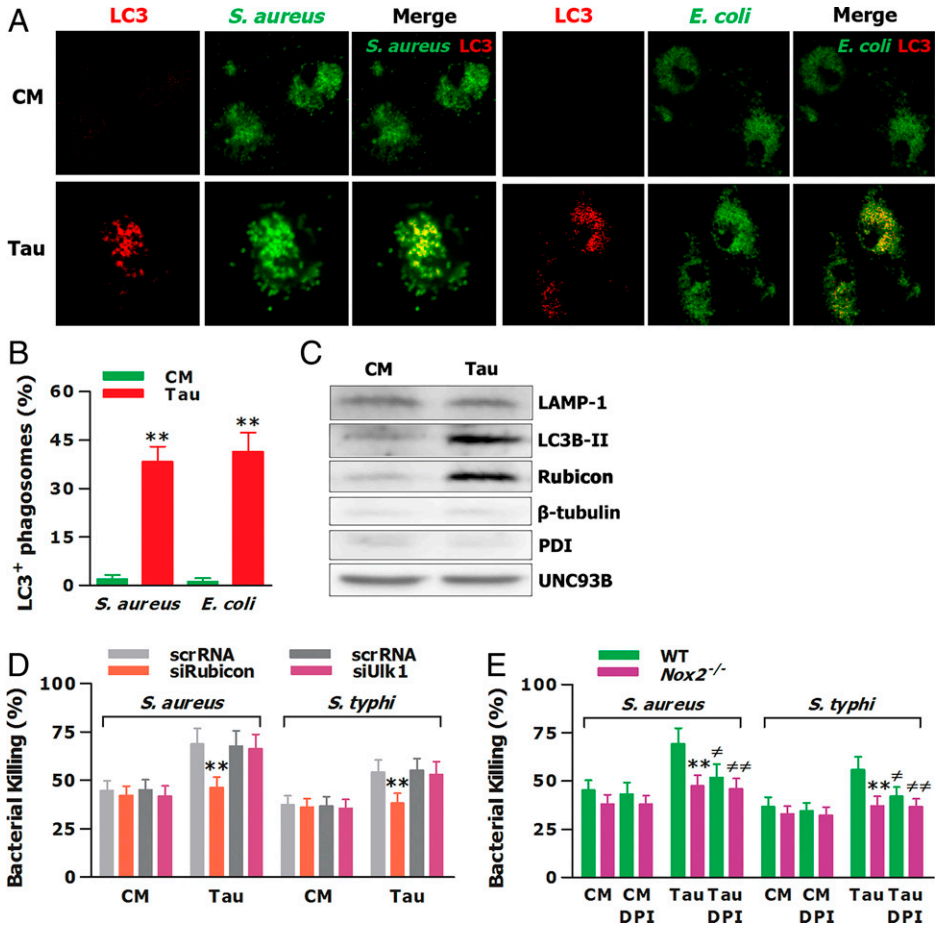

Fig. 6. Tau-initiated LAP in innate phagocytes is critically required for an augmented bactericidal activity. (*A*–*C*) Isolated BMMs were treated with CM or Tau (50 μM) for 12 h and further challenged with FITC-conjugated *S. aureus* and *E. coli* or live *E. coli* for 60 min. The recruitment of LC3 to FITC-*S. aureus*- or FITC-*E. coli*-containing phagosomes was detected after incubation with anti-LC3 antibody (*A*) and expressed as the percentage of $LC3^+$ phagosomes (*B*). Phagosomes were purified from CM-treated or Tau-treated, live *E. coli*-challenged BMMs and analyzed by immunoblotting (*C*). Data in *B* are mean ± SD. $^{**}P < 0.01$ versus CM-treated macrophages. (*D* and *E*) Isolated macrophages were transfected with siRubicon, siUlk1, or their scrRNA for 48 h and then treated with CM or Tau for 12 h (*D*), while macrophages isolated from WT and *Nox2*$^{-/-}$ mice were incubated with PBS or DPI (10 μM) for 2 h and then treated with CM or Tau for 12 h (*E*). All these cells were further challenged with live *S. aureus* and *S. typhimurium* for 2 h to assess intracellular killing. Data in *D* and *E* are mean ± SD (n = 4 to 6 in triplicate). $^{**}P < 0.01$ versus scrRNA-transfected, Tau-treated WT macrophages or Tau-treated WT macrophages; $^{\neq}P < 0.05$, $^{\neq\neq}P < 0.01$ versus Tau-treated WT macrophages in the absence of DPI.

tolerance in taurolidine-treated PECs and IECs. To address this, we blocked the autophagy pathway with 3-MA in PECs and IECs isolated from wild-type mice and also used PECs and IECs isolated from *LC3b*$^{-/-}$ mice. Either pharmacological inhibition of autophagy in wild-type PECs by 3-MA or genetically autophagic deficiency in *LC3b*$^{-/-}$ PECs strongly abrogated or even totally abolished taurolidine-induced attenuation in LPS-induced PEC apoptosis (Fig. 7*I*) and endothelial monolayer permeability (Fig. 7*J*). Similarly, taurolidine-improved cell viability and epithelial monolayer integrity in LPS-challenged IECs were markedly impaired in 3-MA-treated wild-type IECs or completely abrogated in *LC3b*$^{-/-}$ IECs (Fig. 7 *K* and *L*). These results suggest that autophagy induction is the prerequisite for taurolidine-augmented capacity of disease tolerance against LPS-induced cell death and damage to the monolayer integrity in vascular endothelium and gut epithelium.

Discussion

In the current study, we show that taurolidine administered 6 h before CLP as a preventive intervention or 6 h after CLP as a therapeutic regime confers robust protection against CLP-induced severe polymicrobial sepsis. Importantly, we find that this in vivo protection is closely associated with taurolidine-augmented host resistance and disease tolerance when given before the septic challenge, whereas taurolidine-afforded protection is predominantly dependent on enhanced disease tolerance when given after the commencement of infection.

Two evolutionarily conserved yet sharply different defense strategies, namely, host resistance and disease tolerance, have attracted much attention in the research area of microbial infection (7, 8, 41). The resistance strategy depends fully on the host immune system, which reduces microbial pathogen burden by detection, destruction, and elimination of the invaded pathogens (10–12). By contrast, disease tolerance is an emerging defense strategy, which minimizes infection-associated disease severity by attenuation, restraint, and limitation of cell and tissue damage, without directly targeting microbial pathogens (8, 41). To examine whether taurolidine-afforded protection against microbial sepsis is associated with an augmentation in host resistance and/or disease tolerance, we measured bacterial clearance, systemic inflammatory responses, and PMN influx into the infected site to reflect innate-immunity-associated host resistance to microbial infection. We also measured the extent of organ damage and vascular and gut permeability to reflect the capacity of disease tolerance to minimize infection-induced

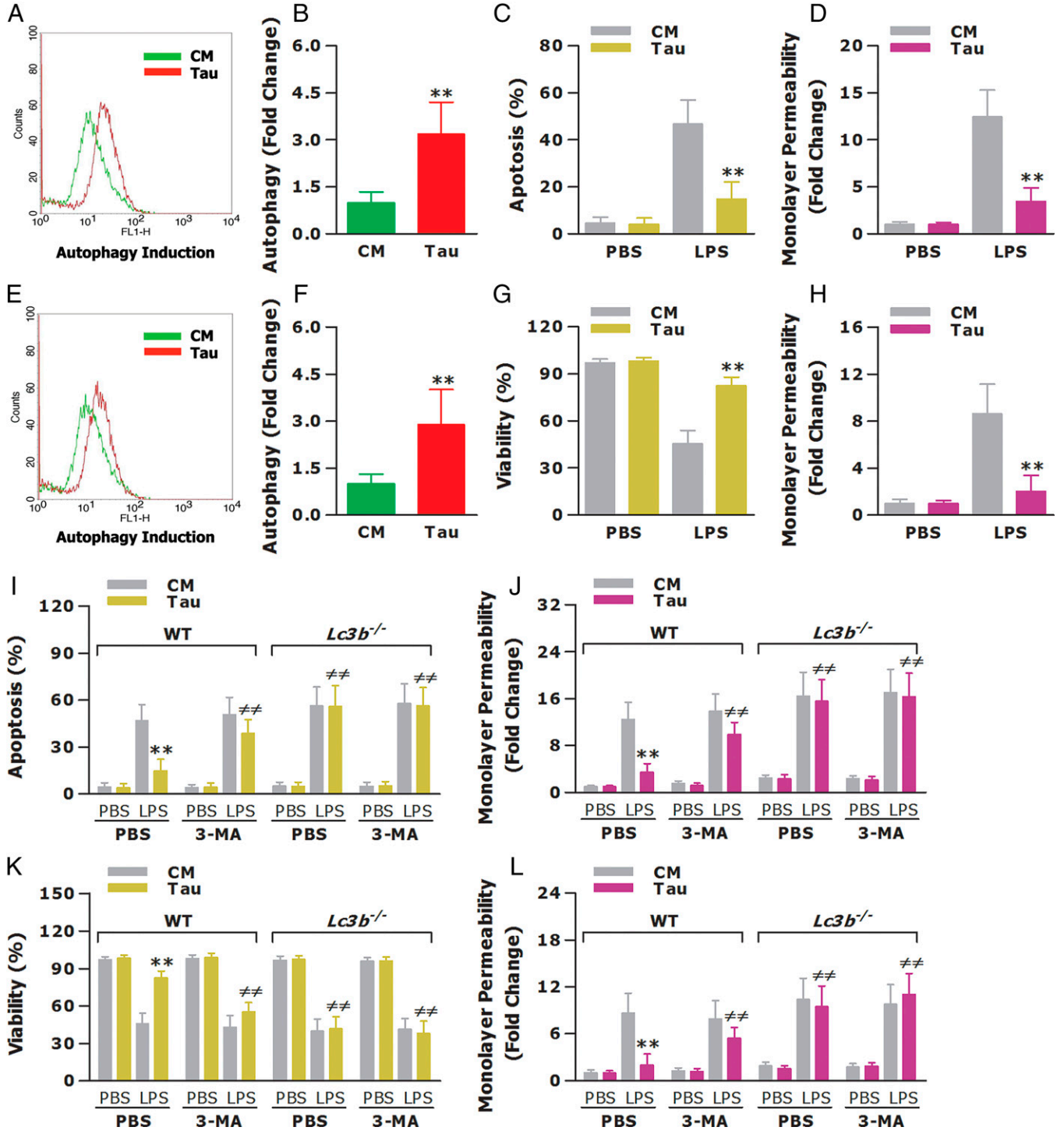

Fig. 7. Tau-induced autophagy attenuates LPS-induced cellular damage in vascular endothelium and gut epithelium by boosting their disease tolerance capacity. (*A–H*) Isolated primary PECs and IECs were treated with CM or Tau (50 μM) for 12 h to induce autophagy (*A*, *B*, *E*, and *F*), and further challenged with PBS or LPS (1.0 or 2.0 μg/mL) for 24 h to assess PEC apoptosis (*C*), IEC viability (*G*), and endothelial (*D*) or epithelial (*H*) monolayer permeability. (*I–L*) Primary PECs and IECs isolated from WT and *LC3b*$^{-/-}$ mice were incubated with PBS or 3-MA (5.0 mM) for 2 h, then treated with CM or Tau (50 μM) for 12 h, and further challenged with PBS or LPS (1.0 or 2.0 μg/mL) for 24 h to assess PEC apoptosis (*I*), IEC viability (*K*), and endothelial (*J*) or epithelial (*L*) monolayer permeability. Autophagy induction and endothelial or epithelial monolayer permeability were expressed as the fold change. Data in *B–D*, *F–H*, and *I–L* are mean ± SD ($n = 4$ to 6 in duplicate or in triplicate). $^{**}P < 0.01$ versus PBS-incubated, CM-treated WT PECs or IECs; $^{\neq\neq}P < 0.01$ versus PBS-incubated, Tau-treated WT PECs or IECs.

disease severity. Administration of taurolidine before the start of infection, i.e., at 6 h before CLP, strongly augmented the capacity of both host resistance and disease tolerance, as supported by accelerated bacterial clearance with significantly reduced bacterial burden in the circulation and visceral organs as well as by ameliorated tissue and organ injury with substantially attenuated vascular and gut permeability. Interestingly, taurolidine administered after the onset of infection, i.e., at 6 h after CLP, did not augment host resistance but potently enhanced disease tolerance to microbial-infection-induced cell and tissue damage with effective organ protection and simultaneous significant reductions in vascular and gut permeability. This therapeutically protective effect of taurolidine via augmentation of the tolerance strategy is consistent with a previous study

where anthracyclines, a group of chemotherapy agents, protected mice against sepsis-related lethality even when given after the initiation of infection, by increasing disease tolerance with substantially ameliorated organ damage (42). Importantly, this protection afforded by either taurolidine, or anthracyclines administered after the onset of infection not only highlights a positive contribution of disease-tolerance-associated organ protection in host defense against microbial sepsis but also emphasizes a potential therapeutic option for septic patients by targeting disease tolerance to prevent further tissue and organ injury, thereby protecting these patients against sepsis-related organ failure (43).

There is increasing evidence to support the importance of autophagy, by functioning as both a self-eating system for the maintenance of cellular homeostasis (17, 19) and an innate "scavenger" by means of xenophagy and LAP for engulfment and killing of the invaded pathogens (21, 25), in host defense against microbial infection (42, 44). To determine whether taurolidine-afforded protection against microbial sepsis relies predominately on autophagy induction, we used autophagy-deficient $LC3b^{-/-}$ mice either subjected to CLP-induced midgrade polymicrobial sepsis or infected with combined *S. aureus* and *S. typhimurium*. We found that $LC3b^{-/-}$ mice were more susceptible to both CLP-induced polymicrobial sepsis and live bacterial infection in comparison with their wild-type littermates. Critically, taurolidine protected wild-type mice but failed to rescue $LC3b^{-/-}$ mice from sepsis-associated lethality. We further assessed bacterial clearance to represent host resistance and organ damage plus vascular and gut permeability to represent disease tolerance, as these parameters were dramatically improved by taurolidine in wild-type mice challenged with CLP-induced high-grade polymicrobial sepsis. Of note, treatment of $LC3b^{-/-}$ mice with taurolidine neither reduced bacterial burden in the circulation and visceral organs nor attenuated organ damage and vascular and gut permeability, indicating that taurolidine is unable to enhance the capacity of both host resistance and disease tolerance in $LC3b^{-/-}$ mice. Similar results were also found in autophagy-deficient $Becn1^{+/-}$ mice where taurolidine failed to protect against microbial sepsis and to augment host resistance and disease tolerance in these mice. Thus, an intact autophagy pathway for autophagy induction is required for taurolidine-induced augmentation in both host resistance and disease tolerance and consequent protection against microbial sepsis. Taurolidine functions as an antibacterial substance (27, 28); therefore, the protection seen in taurolidine-treated septic mice could be also ascribed to taurolidine-associated antibacterial action. To address this, we treated CLP-challenged mice with antibiotics and fluid resuscitation. Surprisingly, antibiotic administration plus fluid resuscitation neither reduced the mortality rate nor attenuated organ damage and vascular and gut permeability in septic mice. Remarkably, taurolidine conferred robust protection with significantly improved overall survival in CLP-challenged, antibiotic-plus-fluid-resuscitation-treated mice, which is predominantly associated with taurolidine-induced augmentation in disease tolerance, as evidenced by effectively ameliorated organ damage and substantially attenuated vascular and gut permeability. Furthermore, a complete loss of protection was observed in CLP-challenged, taurolidine-treated $LC3b^{-/-}$ mice. Together, these results suggest that taurolidine-afforded protection against microbial sepsis observed in the current study is unlikely dependent on its antibacterial effect.

It has been shown that autophagy induction is one of the underlying cellular mechanisms by which taurolidine exerts its multiple functions (31, 32). To clarify whether taurolidine initiates autophagy induction in innate phagocytes, vascular endothelium, and gut epithelium, thereby promoting cellular resistance and tolerance to septic challenges, we treated murine macrophages, PECs, and IECs with taurolidine. Our results revealed that taurolidine induces autophagy in these cells with subsequent increases in engulfment and killing of microbial pathogens in macrophages and significant attenuation in LPS-induced cell death and disruption of endothelial and epithelial monolayers in EPCs and IPCs, indicating augmented capacities of cellular resistance in innate phagocytes and disease tolerance in vascular endothelium and gut epithelium. To determine whether autophagy induction is a critical event for taurolidine-augmented cellular resistance and tolerance in these cells, we blocked the autophagy pathway by using either an autophagy inhibitor 3-MA in wild-type macrophages, EPCs, and IPCs or $LC3b^{-/-}$ macrophages, EPCs, and IPCs. Remarkably, strong attenuation or almost complete abolition in taurolidine-enhanced bactericidal activity was observed in 3-MA-treated wild-type macrophages or $LC3b^{-/-}$ macrophages. Similarly, taurolidine-afforded protection against LPS-induced cell death and monolayer disruption was severely impaired or even totally lost in 3-MA-treated wild-type EPCs and IPCs or $LC3b^{-/-}$ EPCs and IPCs. Thus, an intact autophagy pathway for autophagy induction is required for taurolidine-augmented cellular resistance in innate phagocytes and disease tolerance in vascular endothelium and gut epithelium. Accumulated evidence has revealed that in addition to xenophagy, a canonical autophagy, innate phagocytes can engulf and degrade the invaded microbial pathogens via LAP, a noncanonical autophagy (23–25). To ascertain whether taurolidine preferably induces LAP or xenophagy in innate phagocytes, macrophages were treated with taurolidine and challenged with *S. aureus* or *E. coli*. The observed LC3 recruitment to *S. aureus*- or *E. coli*-containing phagosomes in taurolidine-treated macrophages and detected LC3B-II and Rubicon in phagosomes isolated from taurolidine-treated macrophages indicate that taurolidine initiates LAP specifically in innate phagocytes. Critically, silencing Rubicon or knocking out NOX2, two essential components required for LAP but not for xenophagy, almost completely abolished taurolidine-enhanced intracellular bacterial killing, whereas silencing Ulk1, a constituent essential for xenophagy but dispensable for LAP, failed to attenuate an increased bactericidal activity in taurolidine-treated macrophages, emphasizing that LAP rather than xenophagy accounts predominantly for taurolidine-induced augmentation in innate phagocyte-associated bactericidal activity and subsequent protection against microbial infection. Nevertheless, further investigation using mice deficient in Rubicon is warranted to verify whether taurolidine-afforded protection against microbial sepsis is primarily dependent on LAP.

Together, we demonstrate that taurolidine confers protection against microbial sepsis by promoting both host resistance and disease tolerance. Critically, autophagy induction is the prerequisite for taurolidine-augmented host resistance and disease tolerance and consequent protection. Further work is needed to elucidate the specific pathways and molecular events involved in the link between autophagy and host defense strategies, and in particular the mechanism(s) of disease tolerance.

Materials and Methods

Materials. Reagents used are included in *SI Appendix*.

Polymicrobial Sepsis and Bacterial Infection. C57BL/6 and $LC3b^{-/-}$ mice were subjected to CLP-induced polymicrobial sepsis as described previously (45, 46). Briefly, a midline laparotomy was performed, and ~75% or 40% of the

cecum was ligated to induce either a high-grade or a midgrade polymicrobial sepsis model with an overall mortality rate at ~85% or 35%. A single through-and-through puncture was then made distal to the ligature, and survival rates were monitored for at least 7 d. In some experiments, mice were subjected to CLP-induced high-grade polymicrobial sepsis and received a single intraperitoneal injection of antibiotics imipenem/cilastatin (25 mg/kg body weight) plus a single subcutaneous injection of 0.9% normal saline (30 mL/kg body weight) at 3 h post-CLP (33). Mice treated with taurolidine received an intraperitoneal injection of taurolidine (125 mg/kg body weight) either at 6 h before CLP or at 6 or 12 h after CLP, and mice treated with PBS received an equal volume of PBS (200 μL) intraperitoneally. Mice subjected to sham-CLP underwent the midline laparotomy only. Mice were also infected intraperitoneally with a combination of *S. aureus* at 1×10^7 colony-forming unit (CFU)/mouse and *S. typhimurium* at 1×10^6 CFU/mouse. Survival rates were monitored for at least 14 d.

Measurement of Serum Cytokines, LDH, CK, ALT, and Urea. Mice were subjected to CLP-induced polymicrobial sepsis, and blood samples were collected via retinal artery puncture at different time points post-CLP. Serum TNF-α and IL-6 were assessed by cytometric bead array (BD Biosciences). Serum LDH, CK, ALT, and urea were assessed using EnzyChrom and QuantiChrom assay kits (BioAssay Systems).

Enumeration of Bacteria in the Blood and Visceral Organs. Bacterial counts in the circulation and visceral organs were determined as described previously (45, 47). Briefly, mice were culled at various time periods after CLP. Blood samples were obtained by retinal artery puncture, and the dissected liver, spleen, and lungs were homogenized in sterile PBS. Serial 10-fold dilutions of heparinized whole blood and organ homogenates in sterile water containing 0.5% Triton X-100 (Sigma-Aldrich) were plated on brain heart infusion agar (BD Biosciences) and incubated for 24 h at 37 °C for determination of bacterial CFU.

FACScan Analysis of Peritoneal Macrophage and PMN Subpopulations. Peritoneal lavage was harvested from mice at different time points before and after CLP. Peritoneal exudate cells were incubated with anti-CD11b (BD Pharmingen), anti-CD11c (BioLegend), anti-F4/80 (BD Pharmingen), and anti-Gr1 (BioLegend) monoclonal antibodies (mAbs) conjugated with FITC, PE, PerCP, or APC. FITC-, PE-, PerCP-, and APC-conjugated anti-mouse isotype-matched mAbs (BD Pharmingen; BioLegend) were used as negative controls. Subpopulations of macrophages ($CD11b^+F4/80^-CD11c^{lo}$) and PMNs ($CD11b^+F4/80^-Gr1^{hi}$) in the peritoneal cavity were detected by FACScan analysis (BD Biosciences).

Assessment of Blood Vascular Permeability. The in vivo blood vascular permeability was assessed by an intravenous injection of Evans blue dye (EBD) as described previously (48, 49). Briefly, mice were subjected to CLP-induced polymicrobial sepsis and received an intravenous injection of 200 μL of EBD solution (0.5%) through the tail vein at different time points post-CLP. Mice were sacrificed 30 min after EBD injection to harvest the lungs, liver, and kidneys. The harvested organs were air dried, weighed, and further incubated in formamide (Sigma-Aldrich) at 56 °C for 24 h to extract EBD from each organ. The extracted EBD concentration was spectrophotometrically quantified and expressed as nanograms of EBD per milligram of tissue.

Assessment of Gut Permeability. The gut permeability was assessed by gastric gavage of FITC-conjugated Dextran (4 kDa) (FITC-Dextran), a nonmetabolizable macromolecule, as a permeability probe as described previously (50, 51). Briefly, mice were subjected to CLP-induced polymicrobial sepsis and received gastric gavage of 200 μL of FITC-Dextran solution (100 mg/mL) at different time points post-CLP. Blood samples were collected via retinal artery puncture 4 h after gastric gavage of FITC-Dextran. Serum concentrations of FITC-Dextran were assessed by a Synergy HTX multimode plate reader (BioTec) and calculated based on a serially diluted FITC-Dextran-established standard curve.

Stimulation of Murine Macrophages, PECs, and IECs. Isolated peritoneal macrophages or bone-marrow-derived macrophages (BMMs), primary PECs, and IECs were incubated with CM or taurolidine (50 μM) for 12 h to induce autophagy. They were further challenged with gram-positive or gram-negative bacteria to assess bactericidal activity or challenged with LPS to assess cell damage and permeability of endothelial and epithelial monolayers. Isolated peritoneal macrophages or BMMs, PECs, and IECs were also treated with the autophagy inhibitor 3-MA (5.0 mM) or ROS inhibitor DPI (10 μM) for 2 h before incubation with CM or taurolidine.

Measurement of Autophagy Induction. Isolated peritoneal macrophages or BMMs, primary PECs, and IECs were incubated with CM or taurolidine at the indicated concentrations for various time periods. Autophagy induction was assessed either by FACScan analysis (BD Biosciences) or by a Synergy HTX multimode plate reader (BioTec) after live cells were stained using the Cyto-ID autophagy detection kit (Enzo Life Sciences) according to the manufacturer's instruction.

Assessment of Bacterial Phagocytosis and Killing. Bacterial phagocytosis and intracellular bacterial killing were determined as described previously (45, 47). Briefly, *S. aureus* and *S. typhimurium* were heat killed and labeled with 0.1% FITC (Sigma-Aldrich). Isolated macrophages were pretreated with PBS, 3-MA, or DPI; then incubated with CM or taurolidine; and further challenged with heat-killed, FITC-labeled *S. aureus* and *S. typhimurium* for 30 min to assess bacterial phagocytosis or live *S. aureus* and *S. typhimurium* for 60 and 120 min in the presence or absence of cytochalasin B (5 μg/mL) (Sigma-Aldrich) to assess bacterial killing. Bacterial phagocytosis was assessed by FACScan analysis (BD Biosciences). Intracellular bacterial killing was calculated based on the total and extracellular bacterial killings.

Assays for Cell Apoptosis and Viability. Isolated primary PECs and IECs were pretreated with PBS or 3-MA, then incubated with CM or taurolidine, and further challenged with LPS (2.0 μg/mL) for 24 h. Cell apoptosis in PECs was assessed by FACScan analysis (BD Biosciences) using a FITC Annexin V apoptosis detection kit (BD Pharmingen). Cell viability in IECs was spectrophotometrically determined using a MTT assay kit (Abcam).

Assessment of Endothelial and Epithelial Monolayer Permeability. Isolated PECs and IECs were plated onto the 0.4-μm pore size, collagen-coated upper chamber of 24-well plates (ThermoFisher Scientific) and incubated at 37 °C and 5% CO_2 to form the endothelial or epithelial monolayer. The formed monolayer was pretreated with PBS or 3-MA, then incubated with CM or taurolidine, and further challenged with LPS (1.0 μg/mL) for different time points. At the end of each time point, 150 μL FITC-Dextran (1.0 mg/mL) (Sigma-Aldrich) was added onto the top of the monolayer and incubated for a further 30 min. The endothelial or epithelial monolayer permeability was assessed by measuring the fluorescent intensity of FITC-Dextran that penetrated the low chamber using a Synergy HTX multimode plate reader (BioTec).

Immunofluorescent Staining. Isolated macrophages were plated onto 8-well chamber slides (Lab-Tek, Nunc) at 1×10^5 cells/well, treated with CM or taurolidine for 12 h, and further incubated with FITC-conjugated *S. aureus* or *E. coli* for 60 min. After fixation in 2% paraformaldehyde and permeabilization with 0.1% Triton X-100, cells were incubated overnight at 4 °C with an anti-LC3 antibody (MBL International) and then an Alex Fluor 647-conjugated anti-mouse IgG (ThermoFisher Scientific). Slides were examined under a fluorescent Olympus BX61-TRF microscope (Olympus), and fluorescent images were acquired and analyzed using the cell imaging software (Olympus soft imaging solutions).

Small Interfering RNA (siRNA) Transfection. siRNAs specifically targeting Rubicon or Ulk1 and their scrRNA were obtained from GenePharma. Isolated BMMs were transfected with either siRubicon or siUlk1 for 48 h using Lipofectamine RNAiMax (Invitrogen), and their scrRNAs were used as the nonsilencing control. After transfection, cells were further treated with CM or taurolidine and challenged with live *S. aureus* and *S. typhimurium* to assess intracellular bacterial killing.

Immunoblot Analysis. Visceral organs including the lungs, liver, and kidneys harvested at various time periods were homogenized, lysed, and centrifuged to collect the supernatant containing cytoplasmic proteins. Isolated BMMs were treated with CM or taurolidine for 12 h and allowed to phagocytose *E. coli* for 1 h. Phagosomes were purified using a sucrose gradient as described previously (52), and phagosomal proteins were extracted. Equal amounts of protein extracts were separated on sodium dodecyl-polyacrylamide gels and transblotted onto nitrocellulose membranes (Schleicher & Schuell). The membrane was blocked for 1 h with 0.05% Tween-20 containing 5% nonfat milk and probed overnight at 4 °C with anti-LC3B (Abcam), anti-LAMP-1 (Sigma-Aldrich), anti-Rubicon (Cell

Signaling), anti-β-tubulin (Sigma-Aldrich), anti-PDI (Cell Signaling), and anti-UNC93B (Abcam) antibodies. Blots were then incubated with horseradish-peroxidase-conjugated secondary antibodies, developed with SuperSignal chemiluminescent substrate (Pierce), and captured with an LAS-3000 imaging system (Fujifilm).

Statistical Analysis. All data are expressed as the mean ± SD. Statistical analysis was performed using the log rank test for survival and the ANOVA or Mann–Whitney *U* test for all others with GraphPad software version 5.01 (Prism). Differences were judged to be statistically significant when the *P* value was less than 0.05.

Data Availability. All study data are included in the article and/or *SI Appendix*.

ACKNOWLEDGMENTS. This work was supported by the National Natural Science Foundation of China (Grants 81420108022, 81671967, 81871594, 31670853, and 82172132), the Natural Science Foundation of Jiangsu Province (Grant BK20190053), the Gusu Medical Talent Program of Suzhou (GSWS2019015 and GSWS2020043), and the Pediatric Precise Surgical Clinical Medical Center of Suzhou (SZZXJ201505 and SZLCYXZX202104).

Author affiliations: [a]Institute of Pediatric Research, Children's Hospital of Soochow University, Suzhou 215025, China; [b]Department of Academic Surgery, University College Cork, Cork University Hospital, Cork, Ireland; and [c]Department of Pediatric Surgery, Children's Hospital of Soochow University, Suzhou 215025, China

Author contributions: J.H., M.I., H. Zhou, H.P.R., J.H.W., and J.W. designed research; J.H., M.I., H. Zhou, H. Zhao, F.H., Z.B., and Y.L. performed research; J.H., M.I., H. Zhou, D.P.O., and J.H.W. analyzed data; and J.H., M.I., H. Zhou, H.P.R., J.H.W., and J.W. wrote the paper.

1. M. Singer *et al.*, The third international consensus definitions for sepsis and septic shock (Sepsis-3). *JAMA* **315**, 801–810 (2016).
2. D. C. Angus, T. van der Poll, Severe sepsis and septic shock. *N. Engl. J. Med.* **369**, 840–851 (2013).
3. H. B. Nguyen, D. Smith, Sepsis in the 21st century: Recent definitions and therapeutic advances. *Am. J. Emerg. Med.* **25**, 564–571 (2007).
4. R. S. Hotchkiss, I. E. Karl, The pathophysiology and treatment of sepsis. *N. Engl. J. Med.* **348**, 138–150 (2003).
5. G. S. Martin, D. M. Mannino, S. Eaton, M. Moss, The epidemiology of sepsis in the United States from 1979 through 2000. *N. Engl. J. Med.* **348**, 1546–1554 (2003).
6. C. S. Deutschman, K. J. Tracey, Sepsis: Current dogma and new perspectives. *Immunity* **40**, 463–475 (2014).
7. D. S. Schneider, J. S. Ayres, Two ways to survive infection: What resistance and tolerance can teach us about treating infectious diseases. *Nat. Rev. Immunol.* **8**, 889–895 (2008).
8. R. Medzhitov, D. S. Schneider, M. P. Soares, Disease tolerance as a defense strategy. *Science* **335**, 936–941 (2012).
9. S. Akira, S. Uematsu, O. Takeuchi, Pathogen recognition and innate immunity. *Cell* **124**, 783–801 (2006).
10. E. Kopp, R. Medzhitov, Recognition of microbial infection by Toll-like receptors. *Curr. Opin. Immunol.* **15**, 396–401 (2003).
11. T. D. Kanneganti, M. Lamkanfi, G. Núñez, Intracellular NOD-like receptors in host defense and disease. *Immunity* **27**, 549–559 (2007).
12. R. Medzhitov, Recognition of microorganisms and activation of the immune response. *Nature* **449**, 819–826 (2007).
13. J. F. Schafer, Tolerance to plant disease. *Annu. Rev. Phytopathol.* **9**, 235–252 (1971).
14. J. S. Ayres, N. Freitag, D. S. Schneider, Identification of *Drosophila* mutants altering defense of and endurance to *Listeria monocytogenes* infection. *Genetics* **178**, 1807–1815 (2008).
15. L. Råberg, D. Sim, A. F. Read, Disentangling genetic variation for resistance and tolerance to infectious diseases in animals. *Science* **318**, 812–814 (2007).
16. R. Larsen *et al.*, A central role for free heme in the pathogenesis of severe sepsis. *Sci. Transl. Med.* **2**, 51ra71 (2010).
17. B. Levine, G. Kroemer, Autophagy in the pathogenesis of disease. *Cell* **132**, 27–42 (2008).
18. S. Mostowy, Autophagy and bacterial clearance: A not so clear picture. *Cell. Microbiol.* **15**, 395–402 (2013).
19. P. Lapaquette, A. L. Glasser, A. Huett, R. J. Xavier, A. Darfeuille-Michaud, Crohn's disease-associated adherent-invasive *E. coli* are selectively favoured by impaired autophagy to replicate intracellularly. *Cell. Microbiol.* **12**, 99–113 (2010).
20. B. Levine, N. Mizushima, H. W. Virgin, Autophagy in immunity and inflammation. *Nature* **469**, 323–335 (2011).
21. L. C. Gomes, I. Dikic, Autophagy in antimicrobial immunity. *Mol. Cell* **54**, 224–233 (2014).
22. M. Cemma, J. H. Brumell, Interactions of pathogenic bacteria with autophagy systems. *Curr. Biol.* **22**, R540–R545 (2012).
23. M. A. Sanjuan *et al.*, Toll-like receptor signalling in macrophages links the autophagy pathway to phagocytosis. *Nature* **450**, 1253–1257 (2007).
24. J. Huang *et al.*, Activation of antibacterial autophagy by NADPH oxidase. *Proc. Natl. Acad. Sci. U.S.A.* **106**, 6226–6231 (2009).
25. S. Upadhyay, J. A. Philips, LC3-associated phagocytosis: Host defense and microbial response. *Curr. Opin. Immunol.* **60**, 81–90 (2019).
26. B. L. Heckmann, D. R. Green, LC3-associated phagocytosis at a glance. *J. Cell Sci.* **132**, jcs222984 (2019).
27. D. M. Baker *et al.*, Taurolidine peritoneal lavage as prophylaxis against infection after elective colorectal surgery. *Br. J. Surg.* **81**, 1054–1056 (1994).
28. M. Koldehoff, J. L. Zakrzewski, Taurolidine is effective in the treatment of central venous catheter-related bloodstream infections in cancer patients. *Int. J. Antimicrob. Agents* **24**, 491–495 (2004).
29. M. McCourt, J. H. Wang, S. Sookhai, H. P. Redmond, Taurolidine inhibits tumor cell growth *in vitro* and *in vivo*. *Ann. Surg. Oncol.* **7**, 685–691 (2000).
30. B. S. Sun, J. H. Wang, L. L. Liu, S. L. Gong, H. P. Redmond, Taurolidine induces apoptosis of murine melanoma cells *in vitro* and *in vivo* by modulation of the Bcl-2 family proteins. *J. Surg. Oncol.* **96**, 241–248 (2007).
31. H. Möhler, R. W. Pfirrmann, K. Frei, Redox-directed cancer therapeutics: Taurolidine and Piperlongumine as broadly effective antineoplastic agents (review). *Int. J. Oncol.* **45**, 1329–1336 (2014).
32. R. Stendel *et al.*, The antibacterial substance taurolidine exhibits anti-neoplastic action based on a mixed type of programmed cell death. *Autophagy* **5**, 194–210 (2009).
33. A. J. Lewis *et al.*, Prompt administration of antibiotics and fluids in the treatment of sepsis: A murine trial. *Crit. Care Med.* **46**, e426–e434 (2018).
34. K. Nakahira *et al.*, Autophagy proteins regulate innate immune responses by inhibiting the release of mitochondrial DNA mediated by the NALP3 inflammasome. *Nat. Immunol.* **12**, 222–230 (2011).
35. M. Reed, S. H. Morris, A. B. Owczarczyk, N. W. Lukacs, Deficiency of autophagy protein Map1-LC3b mediates IL-17-dependent lung pathology during respiratory viral infection via ER stress-associated IL-1. *Mucosal Immunol.* **8**, 1118–1130 (2015).
36. X. H. Liang *et al.*, Induction of autophagy and inhibition of tumorigenesis by beclin 1. *Nature* **402**, 672–676 (1999).
37. Y. T. Wu *et al.*, Dual role of 3-methyladenine in modulation of autophagy via different temporal patterns of inhibition on class I and III phosphoinositide 3-kinase. *J. Biol. Chem.* **285**, 10850–10861 (2010).
38. J. Martinez *et al.*, Molecular characterization of LC3-associated phagocytosis reveals distinct roles for Rubicon, NOX2 and autophagy proteins. *Nat. Cell Biol.* **17**, 893–906 (2015).
39. J. Martinez *et al.*, Microtubule-associated protein 1 light chain 3 alpha (LC3)-associated phagocytosis is required for the efficient clearance of dead cells. *Proc. Natl. Acad. Sci. U.S.A.* **108**, 17396–17401 (2011).
40. S. Köster *et al.*, *Mycobacterium tuberculosis* is protected from NADPH oxidase and LC3-associated phagocytosis by the LCP protein CpsA. *Proc. Natl. Acad. Sci. U.S.A.* **114**, E8711–E8720 (2017).
41. P. F. Vale, A. Fenton, S. P. Brown, Limiting damage during infection: Lessons from infection tolerance for novel therapeutics. *PLoS Biol.* **12**, e1001769 (2014).
42. N. Figueiredo *et al.*, Anthracyclines induce DNA damage response-mediated protection against severe sepsis. *Immunity* **39**, 874–884 (2013).
43. R. Medzhitov, Septic shock: On the importance of being tolerant. *Immunity* **39**, 799–800 (2013).
44. A. Gluschko *et al.*, The β_2 integrin Mac-1 induces protective LC3-associated phagocytosis of *Listeria monocytogenes*. *Cell Host Microbe* **23**, 324–337.e5 (2018).
45. J. M. Buckley *et al.*, Increased susceptibility of ST2-deficient mice to polymicrobial sepsis is associated with an impaired bactericidal function. *J. Immunol.* **187**, 4293–4299 (2011).
46. D. Rittirsch, M. S. Huber-Lang, M. A. Flierl, P. A. Ward, Immunodesign of experimental sepsis by cecal ligation and puncture. *Nat. Protoc.* **4**, 31–36 (2009).
47. G. C. O'Brien, J. H. Wang, H. P. Redmond, Bacterial lipoprotein induces resistance to Gram-negative sepsis in TLR4-deficient mice via enhanced bacterial clearance. *J. Immunol.* **174**, 1020–1026 (2005).
48. M. Radu, J. Chernoff, An in vivo assay to test blood vessel permeability. *J. Vis. Exp.* (73), e50062 (2013).
49. M. J. Wick, J. W. Harral, Z. L. Loomis, E. C. Dempsey, An optimized Evans blue protocol to assess vascular leak in the mouse. *J. Vis. Exp.* (139), 57037 (2018).
50. L. Wang *et al.*, Methods to determine intestinal permeability and bacterial translocation during liver disease. *J. Immunol. Methods* **421**, 44–53 (2015).
51. B. R. Li *et al.*, In vitro and in vivo approaches to determine intestinal epithelial cell permeability. *J. Vis. Exp.* (140), 57032 (2018).
52. J. Henault *et al.*, Noncanonical autophagy is required for type I interferon secretion in response to DNA-immune complexes. *Immunity* **37**, 986–997 (2012).